ANALYSIS OF SOME LOCAL CLADDING STRESS CONCENTRATIONS--A PROGRESS REPORT

I-Chih Wang and R. W. Weeks

ARGONNE NATIONAL LABORATORY, ARGONNE, ILLINOIS

The facilities of Argonne National Laboratory are owned by the United States Government. Under the terms of a contract (W-31-109-Eng-38) between the U. S. Atomic Energy Commission, Argonne Universities Association and The University of Chicago, the University employs the staff and operates the Laboratory in accordance with policies and programs formulated, approved and reviewed by the Association.

MEMBERS OF ARGONNE UNIVERSITIES ASSOCIATION

The University of Arizona
Carnegie-Mellon University
Case Western Reserve University
The University of Chicago
University of Cincinnati
Illinois Institute of Technology
University of Illinois
Indiana University
Iowa State University
The University of Iowa
Kansas State University
The University of Kansas
Loyola University
Marquette University
Michigan State University
The University of Michigan
University of Minnesota
University of Missouri
Northwestern University
University of Notre Dame
The Ohio State University
Ohio University
The Pennsylvania State University
Purdue University
Saint Louis University
Southern Illinois University
The University of Texas at Austin
Washington University
Wayne State University
The University of Wisconsin

Printed in the United States of America
Available from
National Technical Information Service
U.S. Department of Commerce
5285 Port Royal Road
Springfield, Virginia 22151
Price: Printed Copy $3.00; Microfiche $0.95

ANL-7852
Reactor Technology

ARGONNE NATIONAL LABORATORY
9700 South Cass Avenue
Argonne, Illinois 60439

ANALYSIS OF SOME LOCAL CLADDING STRESS CONCENTRATIONS--A PROGRESS REPORT

by

I-Chih Wang* and R. W. Weeks

Materials Science Division

October 1971

*Visiting Scientist, summer 1969; Associate Professor of Mechanical Engineering, University of Cincinnati, Cincinnati, Ohio

TABLE OF CONTENTS

LIST OF FIGURES

ANALYSIS OF SOME LOCAL CLADDING STRESS CONCENTRATIONS--A PROGRESS REPORT

by

I-Chih Wang and R. W. Weeks

ABSTRACT

As a first step toward the development of fuel-element failure criteria, a general elasticity solution is derived for a thick cylindrical shell under mechanical-loading conditions that can be expressed in the Fourier Series. Appropriate series are then developed for several loading conditions of interest, namely, radial and tangential loads due to fuel-pellet bambooing, a radial point loading that might result from fuel chips between fuel pellets and the cladding, and a spiral-line loading that is probably due to the spiral-wire wrap. An outline for numerical solution of the corresponding creep deformation problems is also included.

I. INTRODUCTION

Most of the presently available analyses[1-5] of fuel elements use plane-strain assumptions and, therefore, neglect the potential stress and/or thermal concentrations that may be expected to arise during normal reactor operation. These local effects may result from the initial form of the fuel, subsequent fuel cracking, local cladding imperfections, out-of-round effects, or the spiral-wire wrap that separates the fuel elements in a subassembly.

Near the end of the useful lifetime of a fuel element, the stress, strain, and/or thermal concentration effects become the dominant factors in determining both the advent and the mechanism of fuel-element failure. In the analysis of accident situations, which may occur at any time, the mechanism of failure will again be influenced by local stresses and hot spots.

As a first step in developing a better understanding of fuel-element stress concentrations, the elastic shell analysis of the "bambooing," or circumferential clad ridging, problem has been undertaken. In addition, the elastic shell analyses for point and spiral-line loading, corresponding to fuel chips and the spiral-wire wrap, respectively, have been formulated.

Bambooing of the cladding occurs at the fuel-pellet interfaces during reactor cycling. It is caused, at least in part, by the nonuniform expansion

of the fuel pellets, which experience large, radial temperature gradients. Local deformations associated with bambooing are most pronounced in fuel elements subjected to high coolant pressures. The elastic shell analysis used in the bambooing problem also forms the first step in the investigation of the local effects caused by fuel cracking and spiral-wire wrap.

In several experimental studies,[6-9] the bambooing problem has been observed and identified, but only Blair and Veeder[10] appear to have performed any detailed analysis. Blair and Veeder, however, restrict their analysis to circumferential ridging of the fuel-pellet column due to axial end loading only and do not consider resultant cladding deformations. Loads due to spiral-fin-type fuel-element spacers have been treated by Baumann et al.[11]

The bambooing effect of the cladding has been analyzed as follows:

(1) Determination of the magnitude and distribution of the normal and tangential loads applied to an initially undeformed cladding in the vicinity of a pellet-pellet interface, a fuel chip, or the spiral-wire wrap, when the fuel is subjected to internal heating and pushes against the cladding.

(2) Determination of the local stress distribution in the cladding that results from the applied loads.

(3) Determination of the resultant elastic and plastic deformation of the cladding, based upon the stress distribution, empirical constitutive equations for the cladding, and a given fuel temperature and swelling history.

(4) Development of failure criteria, given the loading and deformation history of the cladding.

(5) Verification of analytical approach by means of out-of-reactor experiments using a thermohydraulic testing machine with loads programmed to simulate the cyclic in-reactor loading conditions.

Using the published stress-distribution expressions[12] for (1) and (2), the present report includes the equations necessary to predict the elastic and plastic deformation of the cladding, as defined in (3). The present work is part of a relatively short-term effort where, as will be noted, several expedient assumptions have been used in an attempt to evaluate the potential seriousness of the overall problem. In spite of the current assumptions, however, the solution techniques used will form the basis for a more detailed analysis, if further study is deemed necessary after the near-term results have been reviewed.

In Sec. II, the elasticity solution is developed for a long, thick-wall, cylindrical shell subjected to a relatively arbitrary mechanical loading.

The formulation requires only that the shell loading be expressible in Fourier Series. In Sec. III, Fourier Series are developed for bambooing and spiral-line and point loads. Also, the thermoelastic stresses for a hollow cylinder subjected to radial heat flow are considered for superposition. In Sec. IV, the numerical method of "successive elastic solutions"[13] is outlined. This approach, or isochronous stress-strain curves, can be used to predict an approximation of the plastic strain that results from either of the two cases of cladding loading considered in Sec. III.

II. ELASTICITY SOLUTION FOR A CYLINDRICAL SHELL UNDER ARBITRARY MECHANICAL-LOADING CONDITIONS

A. Equilibrium Equations for Cylindrical Shells with Shear Effects

1. Governing Equations

To establish the governing equilibrium equations for solving the elasticity problem of a right-circular cylindrical shell with periodic loads on the middle surface, consider a shell element as shown in Fig. 1, where the dot and the prime denote $\partial(\ )/\partial\varphi$ and $a\partial(\ )/\partial x$, respectively.[14]. As in the membrane theory, the condition for equilibrium of forces in the x direction becomes

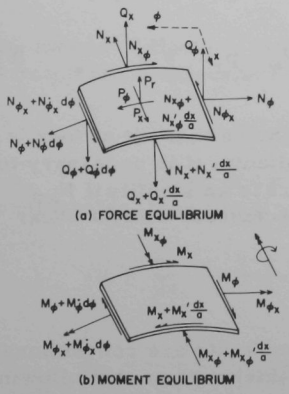

Fig. 1. Shell Element. Neg. No. MSD-55197.

$$a\frac{\partial N_x}{\partial x} + \frac{\partial N_{\varphi x}}{\partial \varphi} + p_x a = 0; \qquad (1)$$

in the φ direction,

$$\frac{\partial N_\varphi}{\partial \varphi} + a\frac{\partial N_{x\varphi}}{\partial x} - Q_\varphi + p_\varphi a = 0; \qquad (2)$$

and the equilibrium equation for the radial components of force is

$$\frac{\partial Q_\varphi}{\partial \varphi} + a\frac{\partial Q_x}{\partial x} + N_\varphi - p_r a = 0. \qquad (3)$$

The equations for equilibrium of moments are

$$\frac{\partial M_\varphi}{\partial \varphi} + a\frac{\partial M_{x\varphi}}{\partial x} - aQ_\varphi = 0 \qquad (4)$$

and

$$a\frac{\partial M_x}{\partial x} + \frac{\partial M_{\varphi x}}{\partial \varphi} - aQ_x = 0. \tag{5}$$

The last condition of equilibrium contains the moments about a radius of the cylinder. Two couples formed by $N_{x\varphi}$ and $N_{\varphi x}$ are the result of the twisting moment $M_{\varphi x}$, so that

$$aN_{x\varphi} - aN_{\varphi x} - M_{\varphi x} = 0. \tag{6}$$

By means of Eqs. 4 and 5, the transverse shears Q_x and Q_φ are eliminated from Eqs. 2 and 3, and we obtain the following in terms of forces and moments:

$$a\frac{\partial N_\varphi}{\partial \varphi} + a\frac{\partial N_{x\varphi}}{\partial x} - \frac{\partial M_\varphi}{\partial \varphi} - a\frac{\partial M_{x\varphi}}{\partial x} + p_\varphi a^2 = 0, \tag{7}$$

and

$$\frac{\partial^2 M_\varphi}{\partial \varphi^2} + a\frac{\partial^2 M_{x\varphi}}{\partial x \partial \varphi} + a\frac{\partial^2 M_{\varphi x}}{\partial x \partial \varphi} + a^2\frac{\partial^2 M_x}{\partial x^2} + aN_\varphi - p_r a^2 = 0. \tag{8}$$

Equations 1 and 6-8 are the governing equations. Since this set of four equations still contains eight unknown stress resultants, it is necessary to consider the deformation of the shell. Actually, Eq. 6 is an identity if $N_{x\varphi}$, $N_{\varphi x}$, and $M_{\varphi x}$ are expressed in terms of the displacements without shear deformation.

2. Stress Resultants

For a circular cylinder, the stress resultants are conventionally defined by the integration of stresses through the thickness as the following:

$$N_x = \int_{-t/2}^{t/2} \sigma_x \left(1 + \frac{z}{a}\right) dz, \tag{9}$$

$$N_\varphi = \int_{-t/2}^{t/2} \sigma_\varphi \, dz, \tag{10}$$

$$N_{x\varphi} = \int_{-t/2}^{t/2} \tau_{x\varphi} \left(1 + \frac{z}{a}\right) dz, \tag{11}$$

$$N_{\varphi x} = \int_{-t/2}^{t/2} \tau_{\varphi x}\, dz, \tag{12}$$

$$M_x = -\int_{-t/2}^{t/2} \sigma_x\left(1 + \frac{z}{a}\right) z\, dz, \tag{13}$$

$$M_\varphi = -\int_{-t/2}^{t/2} \sigma_\varphi z\, dz, \tag{14}$$

$$M_{x\varphi} = -\int_{-t/2}^{t/2} \tau_{x\varphi}\left(1 + \frac{z}{a}\right) z\, dz, \tag{15}$$

and

$$M_{\varphi x} = -\int_{-t/2}^{t/2} \tau_{\varphi x} z\, dz. \tag{16}$$

By means of Hooke's law, these stresses can be determined in terms of the strains and displacements associated with their derivatives.

3. Strains and Stresses

If u, v, and w are the displacement components along the shell coordinates, then the strains are defined[14] as

$$\epsilon_x = \frac{\partial u}{\partial x} - z\frac{\partial^2 w}{\partial x^2}, \tag{17}$$

$$\epsilon_\varphi = \frac{1}{a}\frac{\partial v}{\partial \varphi} - \frac{z}{a}\left(\frac{1}{a+z}\right)\frac{\partial^2 w}{\partial \varphi^2} + \frac{w}{a+z}, \tag{18}$$

and

$$\gamma_{x\varphi} = \left(\frac{1}{a+z}\right)\frac{\partial u}{\partial \varphi} + \left(\frac{a+z}{a}\right)\frac{\partial v}{\partial x} - \frac{\partial w}{\partial \varphi}\left(\frac{z}{a} + \frac{z}{a+z}\right). \tag{19}$$

According to Hooke's law and neglecting σ_z, the stress-strain relations are

$$\sigma_x = \frac{E}{1-\nu^2}(\epsilon_x + \nu\epsilon_\varphi), \tag{20}$$

$$\sigma_\varphi = \frac{E}{1-\nu^2}(\epsilon_\varphi + \nu\epsilon_x), \tag{21}$$

and

$$\tau_{x\varphi} = \frac{E}{2(1+\nu)} \gamma_{x\varphi}. \tag{22}$$

4. Stress Resultants--Displacement Relations and Shear Deformations

Substituting Eqs. 20-22 and 17-19 into Eqs. 9-16, we obtain the stress resultants in terms of displacements and their derivatives. Two constants are defined to simplify the following expressions: the extensional rigidity

$$D = \frac{Et}{1 - \nu^2}, \tag{23}$$

and the bending stiffness

$$K = \frac{Et^3}{12(1 - \nu^2)} \tag{24}$$

Note that D and K depend on both the geometry and the material properties.

Making use of Eqs. 23 and 24, and neglecting higher-order terms of t/a, Eqs. 9-16 become

$$N_x = D\left(\frac{\partial u}{\partial x} + \frac{\nu}{a}\frac{\partial v}{\partial \varphi} + \frac{\nu}{a} w\right) - \frac{K}{a}\frac{\partial^2 w}{\partial x^2}, \tag{25}$$

$$N_\varphi = D\left(\frac{1}{a}\frac{\partial v}{\partial \varphi} + \frac{w}{a} + \nu\frac{\partial u}{\partial x}\right) + \frac{K}{a^3}\left(w + \frac{\partial^2 w}{\partial \varphi^2}\right), \tag{26}$$

$$N_{\varphi x} = \frac{D(1-\nu)}{2}\left(\frac{1}{a}\frac{\partial u}{\partial \varphi} + \frac{\partial v}{\partial x}\right) + \frac{K(1-\nu)}{2a^2}\left(\frac{1}{a}\frac{\partial u}{\partial \varphi} + \frac{\partial^2 w}{\partial x \partial \varphi}\right), \tag{27}$$

$$N_{\varphi x} = \frac{D(1-\nu)}{2}\left(\frac{1}{a}\frac{\partial u}{\partial \varphi} + \frac{\partial v}{\partial x}\right) + \frac{K(1-\nu)}{2a^2}\left(\frac{\partial v}{\partial x} - \frac{\partial^2 w}{\partial x \partial \varphi}\right), \tag{28}$$

$$M_\varphi = K\left(\frac{w}{a^2} + \frac{1}{a^2}\frac{\partial^2 w}{\partial \varphi^2} + \nu\frac{\partial^2 w}{\partial x^2}\right), \tag{29}$$

$$M_x = K\left(\frac{\partial^2 w}{\partial x^2} + \frac{\nu}{a^2}\frac{\partial^2 w}{\partial \varphi^2} - \frac{1}{a}\frac{\partial u}{\partial x} - \frac{\nu}{a^2}\frac{\partial v}{\partial \varphi}\right), \tag{30}$$

$$M_{\varphi x} = \frac{K(1-\nu)}{a}\left(\frac{\partial^2 w}{\partial x \partial \varphi} + \frac{1}{2a}\frac{\partial u}{\partial \varphi} - \frac{1}{2}\frac{\partial v}{\partial x}\right), \tag{31}$$

and

$$M_{x\varphi} = \frac{K(1-\nu)}{a}\left(\frac{\partial^2 w}{\partial x \partial \varphi} - \frac{\partial v}{\partial x}\right). \tag{32}$$

These expressions are derived without considering shear deformation. Thus, the deflections w in Eqs. 29-32 refer only to bending. Denoting this by a subscript b, we have, for Eqs. 29 and 30,

$$M_\varphi = \frac{K}{a^2}\left(w_b + \frac{\partial^2 w_b}{\partial \varphi^2} + a^2\nu\frac{\partial^2 w_b}{\partial x^2}\right), \tag{33}$$

and

$$M_x = \frac{K}{a^2}\left(a^2\frac{\partial^2 w_b}{\partial x^2} + \nu\frac{\partial^2 w_b}{\partial \varphi^2} - a\frac{\partial u}{\partial x} - \nu\frac{\partial v}{\partial \varphi}\right). \tag{34}$$

Considering z and Q_x positive in the same direction (see Fig. 2) because of shear deformation, we have[15]

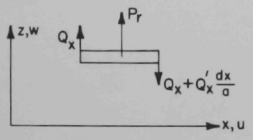

Fig. 2
Shear Forces on a Plate Element. Neg. No. MSD-55198.

$$\frac{\partial w_s}{\partial x} = -1.2\frac{Q_x}{tG}, \tag{35}$$

and, therefore,

$$\frac{\partial^2 w_b}{\partial x^2} = \frac{\partial^2 w}{\partial x^2} - \frac{\partial^2 w_s}{\partial x^2} = \frac{\partial^2 w}{\partial x^2} + 1.2\frac{a^2}{tG}\frac{\partial Q_x}{\partial x}. \tag{36}$$

Similarly, we have

$$\frac{\partial^2 w_b}{\partial \varphi^2} = \frac{\partial^2 w}{\partial \varphi^2} - \frac{\partial^2 w_s}{\partial \varphi^2} = \frac{\partial^2 w}{\partial \varphi^2} + 1.2\frac{a}{tG}\frac{\partial Q_\varphi}{\partial \varphi}. \tag{37}$$

The term w_b indicates the bending moment due to the increase of radius a to $a + w_b$. Substituting Eqs. 36 and 37 into Eqs. 33 and 34, M_φ and M_x become

$$M_\varphi = \frac{K}{a^2}\left[w + \frac{\partial^2 w}{\partial \varphi^2} + \frac{1.2a}{tG}\frac{\partial Q_\varphi}{\partial \varphi} + \nu a^2\left(\frac{\partial^2 w}{\partial x^2} + \frac{1.2a}{tG}\frac{\partial Q_x}{\partial x}\right)\right], \tag{38}$$

and

$$M_x = \frac{K}{a^2}\left[a^2\frac{\partial^2 w}{\partial x^2} + \frac{1.2a^2}{tG}\frac{\partial Q_x}{\partial x} + \nu\left(\frac{\partial^2 w}{\partial \varphi^2} + \frac{1.2a}{tG}\frac{\partial Q_\varphi}{\partial \varphi}\right) - a\frac{\partial u}{\partial x} - \nu\frac{\partial v}{\partial \varphi}\right]. \tag{39}$$

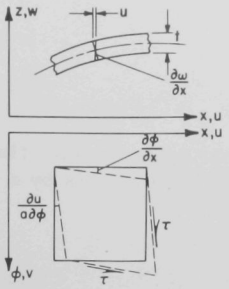

Fig. 3

Shear Strain Resulting from Shear Loads. Neg. No. MSD-55199.

If the shear deflection w_s was due to bending, it would cause outer fiber displacements (see Fig. 3) $u = (-t/2)(\partial w/\partial x)$ and $v = (-t/2a)(\partial w/\partial \varphi)$, and shear strain $\gamma_{x\varphi} = (1/a)(\partial u/\partial x) + (\partial v/\partial x)$. Expressing derivatives of w in terms of the shear forces, as in Eq. 35, this gives $u = (1.2/2)(Q_x/G)$ and $v = (1.2/2)(Q_\varphi/G)$. Then we have

$$\gamma_{x\varphi} = \frac{1.2}{2aG}\left(\frac{\partial Q_x}{\partial \varphi} + a\frac{\partial Q_\varphi}{\partial x}\right). \tag{40}$$

The portion of $M_{\varphi x}$ due to shear will be

$$M_{\varphi xs} = -\frac{t^2}{6}\tau = -\frac{Gt^3}{6}\frac{1.2}{2atG}\left(\frac{\partial Q_x}{\partial \varphi} + a\frac{\partial Q_\varphi}{\partial x}\right). \tag{41}$$

Combining Eq. 41 with Eq. 31 will yield

$$M_{\varphi x} = \frac{K(1-\nu)}{a^2}\left[a\frac{\partial^2 w}{\partial x \partial \varphi} + \frac{1}{2}\frac{\partial u}{\partial \varphi} - \frac{a}{2}\frac{\partial v}{\partial x} + \frac{1.2a}{2tG}\left(\frac{\partial Q_x}{\partial \varphi} + a\frac{\partial Q_\varphi}{\partial x}\right)\right]. \tag{42}$$

Similarly, combining Eq. 41 with Eq. 32 will yield

$$M_{x\varphi} = \frac{K(1-\nu)}{a^2}\left[a\frac{\partial^2 w}{\partial x \partial \varphi} - a\frac{\partial v}{\partial x} + \frac{1.2a}{2tG}\left(\frac{\partial Q_x}{\partial \varphi} + a\frac{\partial Q_\varphi}{\partial x}\right)\right]. \tag{43}$$

The quantity due to shear effect, inside the parentheses of Eqs. 42 and 43, can be expressed as (see Figs. 1 and 4)

$$a\frac{\partial Q_x}{\partial x} + \frac{\partial Q_\varphi}{\partial \varphi} = ap_r - N_\varphi. \tag{44}$$

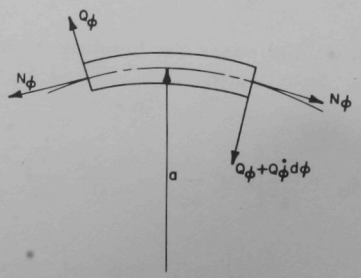

Fig. 4

Shear Force on a Shell Element. Neg. No. MSD-55200.

B. Differential Equations for Displacements

Substituting Eqs. 25-28 and 38, 39, 42, and 43 into Eqs. 1, 7, and 8, and using Eq. 44, we obtain the following fundamental differential equations for the displacements:

$$\frac{\partial^2 u}{\partial x^2} + \frac{1-\nu}{2a^2}(1+k)\frac{\partial^2 u}{\partial \varphi^2} + \frac{1+\nu}{2a}\frac{\partial^2 v}{\partial x \partial \varphi} + \frac{\nu}{a}\frac{\partial w}{\partial x}$$

$$+ k\left(-a\frac{\partial^3 w}{\partial x^3} + \frac{1-\nu}{2a}\frac{\partial^3 w}{\partial x \partial \varphi^2}\right) = -\frac{p_x}{D}, \tag{45}$$

$$\frac{1+\nu}{2a}\frac{\partial^2 u}{\partial x \partial \varphi} + \frac{1}{a^2}\frac{\partial^2 v}{\partial \varphi^2} + \frac{1-\nu}{2}(1+3k)\frac{\partial^2 v}{\partial x^2} + \frac{1}{a^2}\frac{\partial w}{\partial \varphi}$$

$$- \frac{(3-\nu)k}{2}\frac{\partial^3 w}{\partial x^2 \partial \varphi} = -\frac{p_\varphi}{D}, \tag{46}$$

and

$$\frac{\nu}{a}\left(1 - \frac{1.2Dk}{tG}\right)\frac{\partial u}{\partial x} + \frac{k(1-\nu)}{2a}\frac{\partial^3 u}{\partial x \partial \varphi^2} - ak\frac{\partial^3 u}{\partial x^3} + \frac{1}{a^2}\left(1 - \frac{1.2Dk}{tG}\right)\frac{\partial v}{\partial \varphi}$$

$$- \frac{k(3-\nu)}{2}\frac{\partial^3 v}{\partial x^2 \partial \varphi} + k\left(a^2\frac{\partial^4 w}{\partial x^4} + 2\frac{\partial^4 w}{\partial x^2 \partial \varphi^2} + \frac{1}{a^2}\frac{\partial^4 w}{\partial \varphi^4}\right) + \frac{2k}{a^2}\left(1 - \frac{0.6D}{tG}\right)\frac{\partial^2 w}{\partial \varphi^2}$$

$$+ \frac{1}{a^2}\left(1 + k - \frac{1.2Dk^2}{tG}\right)w = \frac{p_r}{D} - \frac{t}{10G}\left(\frac{\partial^2 p_r}{\partial x^2} + \frac{1}{a^2}\frac{\partial^2 p_r}{\partial \varphi^2}\right), \tag{47}$$

where $k = K/Da^2 = t^2/12a^2$.

Equations 45 and 46 are derived without consideration of shear deflections because the effect of shear deflections in these two directions is relatively small.[15] Equation 47 in the radial direction is corrected by adding the shear-deflection terms. The three simultaneous partial differential equations (Eqs. 45-47) may be reduced to a single differential equation in w only. To obtain the complementary solution and the characteristic equation of the shell, let us assume

$$w = C \exp(\lambda x/a) \cos m\varphi. \tag{48}$$

Equation 48 is applicable to most of the loading cases of interest. The characteristic equation can then be obtained as an eighth-order polynomial

of λ with complex roots. The terms u and v will be assumed in the same form as Eq. 48 with constant coefficients to be determined by both substitution and comparison in differential Eqs. 45 and 46.[15] The constant C's can be determined from the boundary conditions on the shell.

C. Particular Solutions for Infinite Shells

For an infinite circular shell, the particular solution with given loading terms is to be determined. Let us assume the loading terms p_r, p_φ, and p_x in trigonometric series form as

$$\left.\begin{aligned} p_x &= p_{xmn} \cos m\varphi \cos \frac{\lambda x}{a} \\ p_\varphi &= p_{\varphi mn} \sin m\varphi \sin \frac{\lambda x}{a} \\ p_r &= p_{rmn} \cos m\varphi \sin \frac{\lambda x}{a} \end{aligned}\right\} \lambda = n\frac{\pi a}{\ell}, \tag{49}$$

where p_{xmn}, $p_{\varphi mn}$, and p_{rmn} are independent constant coefficients. Introducing Eq. 49 into the differential Eqs. 45-47, we see that a particular solution exists in the form

$$\left.\begin{aligned} u &= U_{mn} \cos m\varphi \cos \frac{\lambda x}{a}, \\ v &= V_{mn} \sin m\varphi \sin \frac{\lambda x}{a}, \\ \text{and} \\ w &= W_{mn} \cos m\varphi \sin \frac{\lambda x}{a}, \end{aligned}\right\} \tag{50}$$

where U_{mn}, V_{mn}, and W_{mn} are unknown coefficients. Introducing Eqs. 49 and 50 into Eqs. 45-47 and canceling the trigonometric terms, we arrive at the following set of linear equations for U_{mn}, V_{mn}, and W_{mn}:

$$\begin{bmatrix} A_{11} & A_{12} & A_{13} \\ A_{21} & A_{22} & A_{23} \\ A_{31} & A_{32} & A_{33} \end{bmatrix} \begin{bmatrix} U_{mn} \\ V_{mn} \\ W_{mn} \end{bmatrix} = \frac{a^2}{D} \begin{bmatrix} p_{xmn} \\ p_{\varphi mn} \\ A_{34} p_{rmn} \end{bmatrix}, \tag{51}$$

where

$$A_{11} = \lambda^2 + m^2 \frac{1 - \nu}{2} (1 + k),$$

$$A_{12} = -\frac{1+\nu}{2}\lambda m,$$

$$A_{13} = -\nu\lambda - k\left(\lambda^3 - \frac{1-\nu}{2}\lambda m^2\right),$$

$$A_{21} = -\frac{1+\nu}{2}\lambda m,$$

$$A_{22} = m^2 + \frac{1-\nu}{2}\lambda^2(1+3k),$$

$$A_{23} = m + \frac{3-\nu}{2}k\lambda^2 m,$$

$$A_{31} = -\lambda\nu\left(1 - \frac{1.2Dk}{tG}\right) - k\left(\lambda^3 - \frac{1-\nu}{2}\lambda m^2\right),$$

$$A_{32} = m\left(1 - \frac{1.2Dk}{tG}\right) + \frac{3-\nu}{2}k\lambda^2 m,$$

$$A_{33} = \left(1 + k - \frac{1.2Dk^2}{tG}\right) - 2km^2\left(1 - \frac{0.6D}{tG}\right) + k(\lambda^4 + 2m^2\lambda^2 + m^4),$$

and

$$A_{34} = 1 + \frac{Dt}{10a^2G}(\lambda^2 + m^2).$$

Let B_{ij} be the inverse matrix of A_{ij}. Then

$$\begin{bmatrix} U_{mn} \\ V_{mn} \\ W_{mn} \end{bmatrix} = \frac{a^2}{D}\begin{bmatrix} B_{11} & B_{12} & B_{13} \\ B_{21} & B_{22} & B_{23} \\ B_{31} & B_{32} & B_{33} \end{bmatrix}\begin{bmatrix} p_{xmn} \\ p_{\varphi mn} \\ A_{34}p_{rmn} \end{bmatrix}. \qquad (52)$$

For each value of m and n, the U_{mn}, V_{mn}, and W_{mn} can be expressed in terms of the given loading coefficients p_{xmn}, $p_{\varphi mn}$, and p_{rmn}. The particular solution then will be the summation over all n's and m's.

D. Circular Cylindrical Shells with Axisymmetric Loadings

If the geometry and loading of the circular cylindrical shell are axially symmetric, the equations can be reduced to a simple form. All the terms containing partial derivatives with respect to φ and the terms involving v will be eliminated. Equations 45 and 47 then become

$$\frac{d^2u}{dx^2} + \frac{\nu}{a}\frac{dw}{dx} - ka\frac{d^3w}{dx^3} = -\frac{p_x}{D}, \tag{53}$$

and

$$\frac{\nu}{a}\left(1 - \frac{1.2Dk}{tG}\right)\frac{du}{dx} - ak\frac{d^3u}{dx^3} + ka^2\frac{d^4w}{dx^4}$$

$$+ \frac{1}{a^2}\left(1 + k - \frac{1.2Dk^2}{tG}\right)w = \frac{p_r}{D} - \frac{t}{10G}\frac{d^2p_r}{dx^2}. \tag{54}$$

The loading terms will be

$$p_x = \sum p_{xn} \cos\frac{n\pi x}{\ell} \text{ or } \sum p_{xn} \sin\frac{n\pi x}{\ell}$$

and

$$p_r = \sum p_{rm} \sin\frac{m\pi x}{\ell} \text{ or } \sum p_{rm} \cos\frac{m\pi x}{\ell}. \tag{55}$$

By integration, Eq. 53 becomes

$$\frac{du}{dx} = -\frac{\nu}{a}w + ka\frac{d^2w}{dx^2} - \frac{\bar{p}_x}{D} + C, \tag{56}$$

where $\bar{p}_x = \int p_x\,dx$, and C is an arbitrary constant. Substituting Eq. 56 into Eq. 54, we obtain an ordinary differential equation in terms of w only

$$ka^2(1-k)\frac{d^4w}{dx^4} + k\nu\left(2 - \frac{1.2Dk}{tG}\right)\frac{d^2w}{dx^2} + \frac{1}{a^2}\left[1 + k - \nu^2 + \frac{1.2Dk}{tG}(\nu^2 - k)\right]w$$

$$= \frac{\nu}{a}\left(1 - \frac{1.2Dk}{tG}\right)\left(\frac{\bar{p}_x}{D} - C\right) - \frac{ak}{D}\frac{dp_x}{dx} + \frac{p_r}{D} - \frac{t}{10G}\frac{d^2p_r}{dx^2}, \tag{57}$$

or in the general form,

$$\frac{d^4w}{dx^4} + M\frac{d^2w}{dx^2} + Nw = \sum_{m=1}^{\infty} B_m \sin\frac{m\pi x}{\ell} + \sum_{n=0}^{\infty} E_n \cos\frac{n\pi x}{\ell}, \tag{58}$$

where

$$M = \frac{\nu}{a^2(1-k)}\left(2 - \frac{1.2Dk}{tG}\right),$$

$$N = \frac{1}{ka^4(1-k)}\left[1 + k - \nu^2 + \frac{1.2Dk}{tG}(\nu^2 - k)\right],$$

and

$$B_m \sin\frac{m\pi x}{\ell} + E_n \cos\frac{n\pi x}{\ell}$$

$$= \frac{1}{ka^2(1-k)}\left[\frac{\nu}{a}\left(1 - \frac{1.2Dk}{tG}\right)\left(\frac{\bar{P}_x}{D} - C\right) - \frac{ak}{D}\frac{dp_x}{dx} + \frac{p_r}{D} - \frac{t}{10G}\frac{d^2p_r}{dx^2}\right]. \quad (59)$$

The corresponding displacement will be

$$w = \sum B'_m \sin\frac{m\pi x}{\ell} + \sum E'_n \cos\frac{n\pi x}{\ell}, \quad (60)$$

where

$$B'_m = B_m \Big/ \left[\left(\frac{m\pi}{\ell}\right)^4 - M\left(\frac{m\pi}{\ell}\right)^2 + N\right],$$

and

$$E'_n = E_n \Big/ \left[\left(\frac{n\pi}{\ell}\right)^4 - M\left(\frac{n\pi}{\ell}\right)^2 + N\right]. \quad (61)$$

By means of Eq. 56, the term du/dx can be evaluated as

$$\frac{du}{dx} = -\sum\left[\frac{\nu}{a} + ka\left(\frac{m\pi}{\ell}\right)^2\right] B'_m \sin\frac{m\pi x}{\ell}$$

$$-\sum\left[\frac{\nu}{a} + ka\left(\frac{n\pi}{\ell}\right)^2\right] E'_n \cos\frac{n\pi x}{\ell} - \frac{\bar{P}_x}{D} + C. \quad (62)$$

Then the strains can be evaluated as

$$\epsilon_x = \frac{du}{dx} - z\frac{d^2w}{dx^2},$$

$$\varepsilon_\varphi = \frac{1}{a + z} w,$$

and

$$\gamma_{x\varphi} = 0, \tag{63}$$

and the stresses will be

$$\sigma_x = \frac{E}{1 - \nu^2} (\varepsilon_x + \nu\varepsilon_\varphi)$$

and

$$\sigma_\varphi = \frac{E}{1 - \nu^2} (\varepsilon_\varphi + \nu\varepsilon_x). \tag{64}$$

III. APPLICATIONS OF THE ELASTICITY SOLUTION

A. Periodic Radial Loading for Bambooing

1. Trigonometric Form

Consider a periodic radial loading on the middle surface of the cylindrical shell as

$$\frac{p_r}{p} = p_0 + q_1 \sin \frac{\pi x}{\ell} + p_2 \cos \frac{2\pi x}{\ell} + p_4 \cos \frac{4\pi x}{\ell} + p_6 \cos \frac{6\pi x}{\ell}, \tag{65}$$

where

$$p_0 = 0.318310,$$

$$q_1 = 0.5,$$

$$p_2 = -0.212207,$$

$$p_4 = -0.0424414,$$

and

$$p_6 = -0.0181892.$$

The shape of the periodic loading is shown in Fig. 5. The corresponding radial displacement profile is shown in Fig. 6. The ratio of the loading peak to the displacement peak is $1/[Dka^2(1 - k)]$.

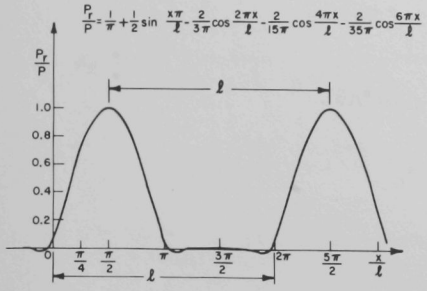

Fig. 5. Radial Surface Load Distribution (trigonometric representation). Neg. No. MSD-55201.

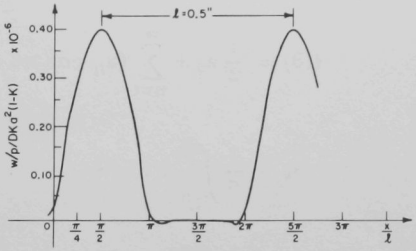

Fig. 6. Radial Displacement Corresponding to Loading Shown in Fig. 5. Neg. No. MSD-55202.

2. Valentin-Carey Normal Load Distribution

The normal surface traction exerted on a cylindrical cladding due to heating of a fuel pellet can be expressed as[12]

$$\sigma_r = p\left\{1 + 1.8\exp\left[-\frac{5\ell}{a}\left(1 - \frac{z}{\ell}\right)\right]\left[\cos\frac{5\ell}{a}\left(1 - \frac{z}{\ell}\right) - \sin\frac{5\ell}{a}\left(1 - \frac{z}{\ell}\right)\right]\right\} \tag{66}$$

for $0 \le z \le \ell$, $\sigma_r(-z) = \sigma_r(z)$,

or

$$\frac{\sigma_r}{p} = 1 + 1.8(\cos\varphi - \sin\varphi)\exp(-\varphi), \tag{67}$$

where $\varphi = 5\ell(1 - z/\ell)/a$. To convert to an even periodic function, let

$$\varphi = \frac{5\ell}{a}\frac{\theta}{\pi};$$

then,

$$\frac{\sigma_r}{p} = 1 + 1.8\left[\cos\left(\frac{5\ell}{\pi a}\theta\right) - \sin\left(\frac{5\ell}{\pi a}\theta\right)\right]\exp\left(\frac{-5\ell}{a\pi}\theta\right), \quad 0 \le \theta \le \pi. \tag{68}$$

Then,

$$f(\theta) = \begin{cases} \dfrac{\sigma_r(\theta)}{p} = 1 + 1.8(\cos k\theta - \sin k\theta)\exp(-k\theta), & 0 \le \theta \le \pi \\ \dfrac{\sigma_r(\theta)}{p} = 1 + 1.8(\cos k\theta + \sin k\theta)\exp(k\theta), & -\pi \le \theta \le 0 \end{cases} \tag{69}$$

where $k = 5\ell/\pi a$. Expanding in Fourier Series,

$$f(\theta) = \frac{1}{2} a_0 + \sum_{n=1}^{\infty} (a_n \cos n\theta + b_n \sin n\theta),$$

$$a_0 = \frac{1}{\pi} \int_{-\pi}^{\pi} f(\theta)\, d\theta,$$

$$a_n = \frac{1}{\pi} \int_{-\pi}^{\pi} f(\theta) \cos n\theta\, d\theta,$$

and

$$b_n = \frac{1}{\pi} \int_{-\pi}^{\pi} f(\theta) \sin n\theta\, d\theta. \tag{70}$$

The first term may be evaluated as

$$a_0 = \frac{1}{\pi} \int_{-\pi}^{\pi} f(\theta)\, d\theta$$

$$= \frac{1}{\pi} \left\{ \int_{-\pi}^{0} [1 + 1.8(\cos k\theta + \sin k\theta) \exp(k\theta)]\, d\theta \right.$$

$$\left. + \int_{0}^{\pi} [1 + 1.8(\cos k\theta - \sin k\theta) \exp(-k\theta)]\, d\theta \right\},$$

which becomes

$$a_0 = 2\left[1 + 1.8\left(\sin \frac{5\ell}{a}\right) \frac{a}{5\ell} \exp(-5\ell/a)\right]. \tag{71}$$

The subsequent a_n terms

$$a_n = \frac{1}{\pi}\left[\int_{-\pi}^{\pi} f(\theta) \cos n\theta\, d\theta = \frac{1}{\pi} \int_{-\pi}^{0} [1 + 1.8(\cos k\theta + \sin k\theta) \exp(k\theta)] \cos n\theta\, d\theta \right.$$

$$\left. + \int_{0}^{\pi} [1 + 1.8(\cos k\theta - \sin k\theta) \exp(-k\theta)] \cos n\theta\, d\theta \right],$$

become

$$a_n = \frac{1.8}{\pi}\left[\frac{n}{k^2 + (k-n)^2} - \frac{n}{k^2 + (k+n)^2}\right.$$

$$- \exp(-k\pi)\frac{(2k-n)\sin(n-k)\pi + n\cos(k-n)\pi}{k^2 + (k-n)^2}$$

$$\left. + \exp(-k\pi)\frac{(2k+n)\sin(k+n)\pi + n\cos(k+n)\pi}{k^2 + (k+n)^2}\right]. \qquad (72)$$

The b_n terms vanish, since $f(\theta)$ is an even function. The Fourier Series approximation for the radial loading is shown in Fig. 7 for n = 20 and n = 50.

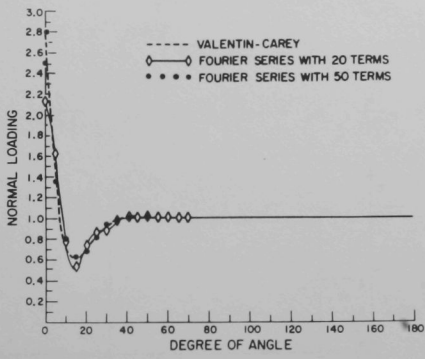

Fig. 7

Valentin-Carey Approximate Normal Surface Loading. Neg. No. MSD-55203.

B. Tangential Loading for Bambooing

1. Linear Form

The linear form of tangential loading can be expressed as (see Fig. 8)

$$\frac{p}{B} = r_1 \cos\frac{\pi x}{\ell} + r_2 \cos\frac{3\pi x}{\ell} + r_3 \sin\frac{2\pi x}{\ell} + r_4 \sin\frac{4\pi x}{\ell}, \qquad (73)$$

where

$$r_1 = \frac{2}{\pi}\left(\frac{2}{\pi} + 1\right), \quad r_2 = \frac{2}{\pi}\left(\frac{2}{9\pi} - \frac{1}{3}\right), \quad r_3 = -\frac{1}{\pi}, \text{ and } r_4 = \frac{1}{2\pi}.$$

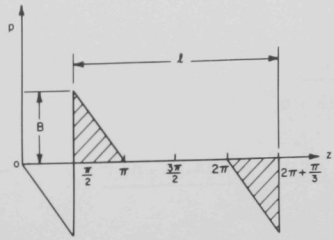

Fig. 8

Linear Form of Tangential Loading. Neg. No. MSD-55204.

2. Trigonometric Form

The trigonometric form of tangential loading can be expressed as (see Fig. 9)

$$\frac{p}{B} = s_1 \cos\frac{\pi x}{\ell} + s_2 \cos\frac{3\pi x}{\ell} + s_3 \cos\frac{5\pi x}{\ell} + s_4 \sin\frac{2\pi x}{\ell} + s_5 \sin\frac{4\pi x}{\ell}, \quad (74)$$

where

$$s_1 = -\frac{1}{\pi}, \quad s_2 = \frac{1}{\pi}, \quad s_3 = -\frac{1}{3\pi}, \quad s_4 = -\frac{4}{3\pi}, \quad \text{and} \quad s_5 = \frac{8}{15\pi}.$$

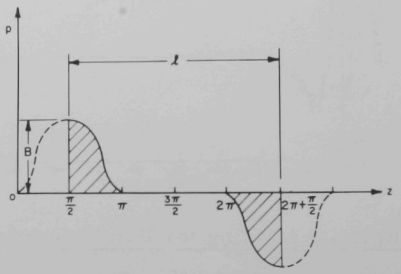

Fig. 9

Trigonometric Form of Tangential Loading. Neg. No. MSD-55205.

3. Valentin-Carey Tangential Surface Loading

According to Carey and Valentin,[12] an approximation of the tangential surface loading for bambooing is

$$\frac{\tau_{rz}}{p} = -31.0\left(\frac{z}{\ell}\right)^3\left[\left(\frac{z}{\ell}\right)^4 - 1\right]^2, \quad -\ell \le z \le \ell. \quad (75)$$

This may be further approximated as

$$f(\theta)\begin{cases} = 0 & \text{for } -\pi < \theta < \frac{\pi}{2}, \\ = \theta\left(\frac{\pi}{2} - \theta\right)\left(\frac{\pi}{2} + \theta\right) & \text{for } -\frac{\pi}{2} < \theta < \frac{\pi}{2}, \\ = 0 & \text{for } \frac{\pi}{2} < \theta < \pi. \end{cases}$$

Representing this in Fourier Series,

$$f(\theta) = \left(\frac{\pi^2}{4} - \theta^2\right)\theta = \sum_{n=1}^{\infty} b_n \sin n\theta, \tag{76}$$

since $f(\theta)$ is an odd function with average value zero, where

$$b_n = \frac{1}{\pi}\int_{-\pi/2}^{\pi/2} f(\theta) \sin n\theta \, d\theta.$$

Then,

$$b_n = \frac{1}{\pi}\int_{-\pi/2}^{\pi/2}\left(\frac{\pi^2}{4}\theta - \theta^3\right)\sin n\theta \, d\theta$$

$$= \frac{1}{\pi}\left(\frac{12}{n^4} - \frac{\pi^2}{n^2}\right)\sin\frac{n\pi}{2} - \frac{6}{n^3}\cos\frac{n\pi}{2}; \tag{77}$$

therefore

$$b_1 = \frac{1}{\pi}(12 - \pi^2) = 0.67813, \quad b_2 = +\frac{6}{8} = 0.75, \quad b_3 = 0.30191,$$

$$b_4 = -0.09375, \quad b_5 = -0.11955, \text{ and } b_6 = 0.027778.$$

Let us normalize b_n by dividing by 1.529396, which is the maximum of $f(\theta)$. Then we have

$$f(\theta) = 0.4434 \sin\theta + 0.4904 \sin 2\theta + 0.1974 \sin 3\theta - 0.0613 \sin 4\theta$$

$$-0.0782 \sin 5\theta + 0.0182 \sin 6\theta. \tag{78}$$

The shear distribution can then be converted to θ as

$$\frac{\tau_{rz}}{6.188p} = f(\theta) = \sum_{n=1}^{6} f_n \sin n\theta. \tag{79}$$

The Fourier Series approximation for the tangential loading is shown in Fig. 10 for n = 6.

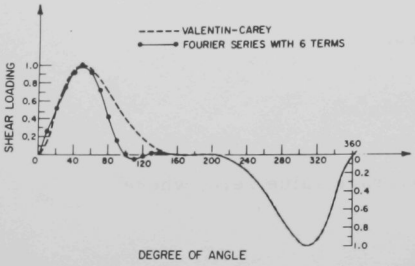

Fig. 10

Valentin-Carey Approximate Shear Surface Loading. Neg. No. MSD-55206.

C. Fourier Analysis of Spiral and Point Loadings on a Cylindrical Surface

The configuration of interest is shown in Fig. 11 along with the coordinate system.

The cylindrical surface is expanded into a rectangular sheet as shown in Fig. 12. The loading on the rectangular surface will be a line load along one of the diagonals of the rectangular sheet.

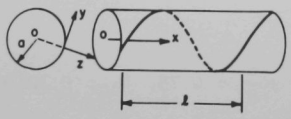

Fig. 11

Coordinate System for Spiral-wire Wrap. Neg. No. MSD-55207.

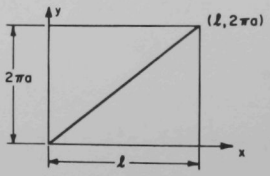

Fig. 12

Cylinder Unrolled into a Flat Sheet. Neg. No. MSD-55208.

1. Point Loading

If a point load on a rectangular plane is considered as q = f(x,y), then the function f(x,y) can be expressed as a double trigonometric series

$$f(x,y) = \sum_{m=1}^{\infty} \sum_{n=1}^{\infty} a_{mn} \sin \frac{m\pi x}{a} \sin \frac{n\pi y}{b}. \tag{80}$$

To calculate any particular coefficient a_{rs} of this series, we multiply both sides by $\sin(s\pi y/b)\,dy$ and integrate from 0 to b. Observing that

$$\int_0^b \sin\frac{n\pi y}{b}\sin\frac{s\pi y}{b}\,dy = \begin{cases} 0 & \text{when } n \neq s \\ b/2 & \text{when } n = s \end{cases}$$

yields

$$\int_0^b f(x,y)\sin\frac{s\pi y}{b}\,dy = \frac{b}{2}\sum_{m=1}^{\infty} a_{ms}\sin\frac{m\pi x}{a}. \tag{81}$$

Multiplying both sides of the equation by $\sin(r\pi x/a)\,dx$ and integrating from 0 to a, we obtain

$$\int_0^a\int_0^b f(x,y)\sin\frac{r\pi x}{a}\sin\frac{s\pi y}{b}\,dx\,dy = \frac{ab}{4}a_{rs},$$

and, therefore,

$$a_{rs} = \frac{4}{ab}\int_0^a\int_0^b f(x,y)\sin\frac{r\pi x}{a}\sin\frac{s\pi y}{b}\,dx\,dy. \tag{82}$$

Applying this result for a single load p that is uniformly distributed over a small rectangular area (see Fig. 13), we have

$$a_{mn} = \frac{4p}{abuv}\int_{\xi-u/2}^{\xi+u/2}\int_{\eta-v/2}^{\eta+v/2}\sin\frac{m\pi x}{a}\sin\frac{n\pi y}{b}\,dx\,dy$$

$$= \frac{16p}{\pi^2 mnuv}\sin\frac{m\pi\xi}{a}\sin\frac{n\pi\eta}{b}\sin\frac{m\pi u}{2a}\sin\frac{n\pi v}{2b}. \tag{83}$$

Taking the limit $u \to 0$ and $v \to 0$, we have

$$a_{mn} = \frac{4p}{ab}\sin\frac{m\pi\xi}{a}\sin\frac{n\pi\eta}{b}. \tag{84}$$

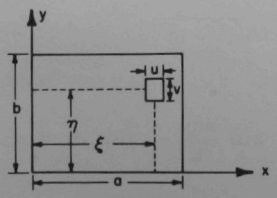

Fig. 13

Coordinate System for Locally Distributed Load. Neg. No. MSD-55209.

For a given value of (ξ,η), the loading function will be

$$q = f(x,y,\xi,\eta) = \sum_{m=1}^{\infty}\sum_{n=1}^{\infty} \frac{4p}{ab} \sin\frac{m\pi\xi}{a} \sin\frac{n\pi\eta}{b} \sin\frac{m\pi x}{a} \sin\frac{n\pi y}{b}. \qquad (85)$$

If we assume $a = \ell$ and $b = 2\pi a_0$, we can convert the result to a circular cylindrical surface with periodic point loads, as shown in Fig. 14. If ℓ is assumed to be sufficiently longer than the diameter of the cylinder, we may consider this example as a circular cylindrical surface with a concentrated radial point load.

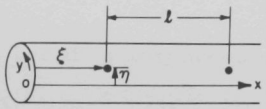

Fig. 14

Coordinate System for Point Loading. Neg. No. MSD-55210.

2. Line Loading

If the w coordinate is set along the diagonal of the line load (see Fig. 15) and if an arbitrary point is located on the line at (ξ,η), then we have

(a) $\tan\theta = \frac{b}{a}$ or $\theta = \tan^{-1}\frac{b}{a}$,

(b) $\xi = w\cos\theta$,

$\eta = w\sin\theta$,

and

(c) the loading function

$$q = \int_0^{\sqrt{a^2+b^2}} f(x,y,\xi,\eta)\, dw, \qquad (86)$$

or

$$q = \sum\sum \frac{4p}{ab} \sin\frac{m\pi x}{a} \sin\frac{n\pi y}{b} \int_0^{\sqrt{a^2+b^2}} \sin\frac{m\pi\xi}{a} \sin\frac{n\pi\eta}{b}\, dw$$

$$= \sum\sum \frac{4p}{ab} \sin\frac{m\pi x}{a} \sin\frac{n\pi y}{b} \frac{\sqrt{a^2+b^2}}{2}$$

$$= \sum\sum \frac{2p\sqrt{a^2+b^2}}{ab} \sin\frac{m\pi x}{a} \sin\frac{n\pi y}{b} \quad \text{for } m = n$$

or finally,

$$q = \sum_{m=1}^{\infty} \frac{2p\sqrt{a^2 + b^2}}{ab} \sin \frac{m\pi x}{a} \sin \frac{m\pi y}{b} . \tag{87}$$

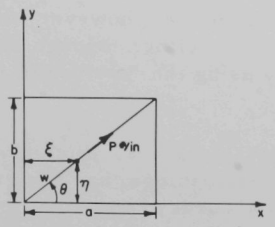

Fig. 15

Coordinate System for Diagonal-line Loading. Neg. No. MSD-55211.

3. Remarks

The expression q may not converge outside the region of interest, but, for engineering purposes, it should be a good approximation for the line loading. When a numerical procedure is used to evaluate the stresses and strains, the approximation should always be convergent.

D. Thermal-stress Distribution

For a cylinder subjected to radial heat flow, the thermoelastic stress distribution is given by[16]

$$\sigma_r = \frac{\alpha E \Delta T}{2(1 - \nu) \ln (b/a)} \left[-\ln \frac{b}{r} - \frac{a^2}{b^2 - a^2} \left(1 - \frac{b^2}{r^2} \right) \ln \frac{b}{a} \right],$$

$$\sigma_\theta = \frac{\alpha E \Delta T}{2(1 - \nu) \ln (b/a)} \left[1 - \ln \frac{b}{r} - \frac{a^2}{b^2 - a^2} \left(1 + \frac{b^2}{r^2} \right) \ln \frac{b}{a} \right],$$

and

$$\sigma_z = \frac{\alpha E \Delta T}{2(1 - \nu) \ln (b/a)} \left(1 - 2 \ln \frac{b}{r} - \frac{2a^2}{b^2 - a^2} \ln \frac{b}{a} \right), \tag{88}$$

where ΔT is the temperature of the inner surface minus the temperature at the outer surface, and α is the coefficient of thermal expansion. For small deformations, this solution may be superimposed on the stresses that result from the mechanical loading. However, local thermal variations, i.e., due to the spiral-wire wrap, remain neglected.

IV. CREEP DEFORMATION ANALYSIS

Since the actual cladding deformations occur at elevated temperatures, the preceding elastic solutions can give only a rough indication of the true behavior of the cladding. In fact, by themselves, the elastic solutions serve only as a limiting-case check for more general inelastic solutions. The elastic solutions may be supplemented, however, to estimate the inelastic deformations. This can be done either through the use of isochronous stress-strain curves, or by using the "method of successive elastic solutions."[13]

The use of isochronous stress-strain curves, which give the total strain at various times for constant stress loadings, has the great advantage of simplicity, although the method lacks accuracy, and usually the creep data required for construction of the curves are not available. For AISI Type 304 or 316 stainless steel, however, isochronous stress-strain curves are available,[17] and these materials are commonly used for fast-reactor fuel-element cladding. It may also be argued that this type of simplified inelastic analysis would be justified since other assumptions already have been made (see Sec. V), and since the goal of the present analysis is only to assess the relative importance of the problem.

Cladding bambooing is intensified, however, by thermal cycling, and a method to predict creep deformations resulting from a prescribed thermal and mechanical loading history is necessary for a more accurate assessment of the total deformation. The method of successive elastic solutions is appropriate to this objective, although difficult to implement, even for the simple geometry considered here. To use this incremental numerical method, inelastic deformation terms representing the total accumulated plastic deformation and the increment of deformation appropriate to the time step must be included in the constitutive relations. An empirical cladding creep law is used in conjunction with a flow rule to obtain the inelastic deformation increment. The constitutive relations are then combined with the usual field equations and solved iteratively, since the stress depends on the strain increment and the strain increment depends on the stress. Examples of the use of this method have been presented elsewhere.[1,13]

An elastic-plastic, finite-element or finite-difference procedure would use the elastic solutions developed here only as a check for the limiting case of elastic behavior. These numerical techniques, however, as well as the method of successive elastic solutions, require considerable amounts of computer time, and the treatment of cyclic loading under creep conditions by finite-element techniques has not been accomplished to date.

In summary, to achieve the final goal of the analysis, namely, an assessment of the possible importance of the various local cladding loads considered, the elastic solution developed in the present report must be

solved numerically and combined with a procedure for estimating the inelastic deformations. The procedure most readily used for this purpose appears to be isochronous stress-strain curves. If the results indicate potentially serious problems, the effort involved in a more detailed analysis, coupled with an experimental program, may be justified.

V. DISCUSSION OF MAJOR ASSUMPTIONS

The internal loading on the cladding due to the fuel will certainly change, not only because of changes in operating conditions but because of the changes in the fuel geometry that result from fuel cracking, swelling, and creep. These load changes due to fuel deformations have been neglected. The loading will also be affected by the cladding deformations, and, if the local cladding deformations become significant in comparison with the global strains, the assumption of a right-circular, cylindrical geometry, upon which the solution in Sec. II is based, becomes questionable. Cladding swelling during irradiation and local thermal variations have also been neglected. In the supplementary inelastic analysis proposed in Sec. IV, sparse uniaxial creep data must often be used to predict strains under multiaxial loading conditions, and a hardening law must be assumed. A creep-law formulation involving primary creep and/or fluence effects must be assumed, even though such a formulation is, at present, only poorly known. The analysis must therefore be viewed as only a first step toward the understanding of a very complex problem, and even predictions made for unirradiated cladding subjected to monotonic loadings must be supplemented by experimental tests.

REFERENCES

1. V. Z. Jankus and R. W. Weeks, *LIFE-I, A FORTRAN-IV Computer Code for the Prediction of Fast-reactor Fuel-element Behavior*, ANL-7736 (Nov 1970).

2. V. Z. Jankus, *BEMOD: A Code for the Lifetime of Metallic Fuel Elements*, ANL-7586 (July 1969).

3. T. R. Bump, *SWELL-2: A Fuel-Element Lifetime Code*, draft dated Oct 16, 1968. (Copies available from author.)

4. C. M. Friedrich and W. H. Guilinger, *CYGRO-2, A Fortran IV Computer Program for Stress Analysis of the Growth of Cylindrical Fuel Elements with Fission-Gas Bubbles*, WAPD-TM-547 (Nov 1966).

5. Y. S. Pan, *A Numerical Solution for the Mechanical Behavior of Cylindrical Fuel Elements*, ASME 68-Wa/NE-14 (1969).

6. H. Fenech and H. M. Gueron, *Circumferential Clad Ridging at Fuel-Pellet Interfaces*, J. Nucl. Appl. *3*, 406 (July 1967).

7. A. Ridal and A. S. Bain, *Irradiation of UO_2 Fuel Elements to Study Circumferential Ridging of the Sheath*, CRFD-1074 (AECL-1463) (Feb 1962).

8. G. Kjaesheim and E. Rolstad, *In-core Study of Fuel/Clad Interaction and Fuel Centre Temperature*, OECD Halden Reactor Project, Halden, Norway (to be published).

9. W. H. Etz, *Fuel Rod Deformation in the SPERT-III Oxide E-Core*, IDO-17291 (Jan 1969).

10. J. M. Blair and J. I. Veeder, *The Elastic Deformation of a Circular Rod of Finite Length for an Axially Symmetric End Face Loading*, J. Appl. Mech. *36*, 241-246 (1969).

11. W. Baumann, V. Casal, H. Hoffmann, R. Moeller, and K. Rust, *Fuel Elements with Spiral Spacers for Fast Breeder Reactors*, KFK 768, EURFNR-571 (Apr 1968).

12. J. J. Carey and R. A. Valentin, "On Thermal Stresses in Clad Pellet Stacks and the Problem of Interface Stress States," *Proc. First Intl. Conf. on Structural Mechanics in Reactor Technology*, Berlin, 1971 (to be published).

13. A. Mendelson, *Plasticity: Theory and Application*, Macmillan Company, New York, Chapt. 9 (1968).

14. W. Flügge, *Stresses in Shells*, Springer-Verlag, Berlin (1960).

15. P. P. Bijlaard, R. J. Dohrmann, and I. C. Wang, *Stresses in Junction of Nozzle to Cylindrical Pressure Vessel for Equal Diameter of Vessel and Nozzle*, Nucl. Eng. Design *5*(3), 349 (May 1967).

16. S. Timoshenko and J. N. Goodier, *Theory of Elasticity*, McGraw-Hill Book Company, Inc., New York, 2nd Ed. (1951).

17. A. L. Snow and M. Jakub, *Interim Supplementary Structural Design Criteria for Elevated Temperatures*, WADCO, FRA-152, Revision 3 (Nov 1970).